

DPGAN: A Dual-Path Generative Adversarial Network for Missing Data Imputation in Graphs

Xindi Zheng¹, Yuwei Wu², Yu Pan³, Wanyu Lin^{1†}, Lei Ma^{4,5}, Jianjun Zhao³

¹Hong Kong Polytechnic University

²National University of Singapore

³Kyushu University

⁴University of Alberta

⁵University of Tokyo

{xin-di.zheng, wan-yu.lin}@polyu.edu.hk, yw.wu@nus.edu.sg, panyu.ztj@gmail.com, lei.ma@acm.org, zhao@ait.kyushu-u.ac.jp

Abstract

Missing data imputation poses a paramount challenge when dealing with graph data. Prior works typically are based on feature propagation or graph autoencoders to address this issue. However, these methods usually encounter the over-smoothing issue when dealing with missing data, as the graph neural network (GNN) modules are not explicitly designed for handling missing data. This paper proposes a novel framework, called Dual-Path Generative Adversarial Network (DPGAN), that can deal simultaneously with missing data and avoid over-smoothing problems. The crux of our work is that it admits both global and local representations of the input graph signal, which can capture the long-range dependencies. It is realized via our proposed generator, consisting of two key components, i.e., MLPUNet++ and GraphUNet++. Our generator is trained with a designated discriminator via an adversarial process. In particular, to avoid assessing the entire graph as did in the literature, our discriminator focuses on the local subgraph fidelity, thereby boosting the quality of the local imputation. The subgraph size is adjustable, allowing for control over the intensity of adversarial regularization. Comprehensive experiments across various benchmark datasets substantiate that DPGAN consistently rivals, if not outperforms, existing state-of-the-art imputation algorithms. The code is provided at <https://github.com/momoxia/DPGAN>.

1 Introduction

Graph-structured data has been widely used to model various relationships for many real-world tasks such as traffic status forecasting [Li *et al.*, 2017], weather prediction [Ni *et al.*, 2022], and molecular classification [Wieder *et al.*, 2020]. However, missing graph attributes is a common issue due to

† denotes the corresponding author.

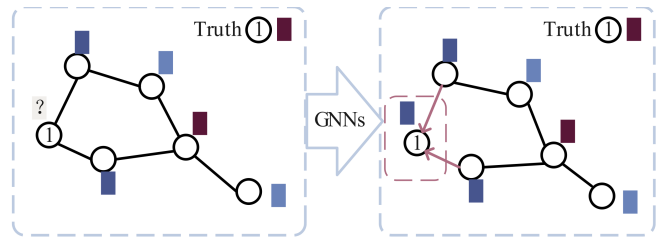


Figure 1: GNNs typically impute missing values by leveraging information from the neighboring nodes. In the graph, node 1 incorrectly imputed a missing value, which could be attributed to the influence of its neighboring nodes.

the chaotic nature of the data collection process [Yoon *et al.*, 2016]. For instance, data might be missing in a biochemical context because of the inherent difficulties of measuring or calculating quantitative molecular properties at an atomic scale ([Yomogida *et al.*, 2012]).

Recent graph-learning-based methods have shown significant progress in addressing the above challenges. GCMF [Taguchi *et al.*, 2021] and FP [Rossi *et al.*, 2022] employ feature propagation for imputation purposes, both of which highly depend on the propagation of local information, inducing sub-optimum solutions. GDN [Li *et al.*, 2020] develops a graph deconvolution operation for recovering graph features from smoothed representations. MEGAE [Gao *et al.*, 2023] attempts to address the spectral concentration problem by maximizing the graph’s spectral entropy. These two works use autoencoders to compress node features into a latent space and then map them back to the original topology for imputation. While these autoencoders are promising, the generated results might be further improved through adversarial training, as shown in [Spinelli *et al.*, 2020]. Though GINN [Spinelli *et al.*, 2020] constructs a graph-based generator and discriminator, it neglects the over-smoothing issue and exhibits instability for high-quality graph feature generation.

To address these gaps, our framework, consisting of a dual-path generator and a subgraph discriminator, is designed to augment the strengths and mitigate the weaknesses of tradi-

tional methods. We recognize that existing GNNs, while proficient in prediction, often falter in feature imputation. This leads to a competency mismatch between generators and discriminators in adversarial training, affecting overall efficacy. In this work, we introduce a novel dual-path model within graph feature generative adversarial networks (GANs) tailored to maintain stable performance across different rates of missing data. Our dual-path approach, comprising the GraphUnet++ and the MLPUnet++, offers a synergistic solution.

The first component of our dual-path generator is GraphUnet++, an innovative MLP-augmented GNN. Building upon the GraphUnet framework [Gao and Ji, 2019], it integrates GNNs for structural data processing with graph pooling layers for downsampling and a graph unpool layer for accurate reconstruction. This process efficiently reduces redundancy in feature and structural information by mapping larger graphs to a more compact graph latent space. A pivotal innovation in GraphUnet++ is the integration of Node-mix MLP layers following GNNs. These layers address the limitations of GNNs in capturing long-range dependencies, enhancing the global representation capabilities of GraphUnet++ for more effective feature imputation.

Complementing GraphUnet++, MLPUnet++ is our second path. Recognizing that traditional GNNs often struggle to capture global graph feature information, especially at lower missing data rates, MLPUnet++ utilizes Node-Mix MLP to facilitate node interactions and Feature-Mix MLP for feature interplay. Besides, the Node-Mix MLP condenses the node dimension to reduce redundancy between nodes. Integrating these two paths in a model ensemble framework allows each to focus on distinct aspects of graph feature learning, significantly enhancing model robustness across various missing data scenarios.

Finally, we propose a subgraph discriminator to further refine the generative process. This unique discriminator, operating on subgraphs of varying sizes, facilitates a balanced training process and enables the generator to undergo adversarial regularization at a suitable intensity, addressing the limitations of traditional single-output discriminators in balancing generator and discriminator capabilities.

Our contributions are as follows:

- We propose the MLP-augmented GraphUnet (GraphUnet++). Traditional adversarial training with only GNNs faces the problem of oversmoothness, which weakens the generator’s capability. To address this issue, we introduce Node-Mix MLP to solve the training problems of graph GANs. The introduction of Node-Mix MLP also enhances the model’s ability to capture long-range dependencies to a certain extent.
- We develop MLPUnet++, a new parallel model branch that further enhances the proposed method in terms of global feature representation, which is designed to capture long-range dependencies more stably. Experiments demonstrate that MLPUnet++ plays a supportive role at low missing rates.
- We propose a subgraph adversarial training strategy, optimizing the performance of a graph-learning-based generator. This is the first GAN model tailored for graph

features, applied to tackle the issue of graph feature imputation. The proposed framework achieves the best performance across various feature-missing rates and datasets.

2 Related Work

2.1 Graph Autoencoder

Since the introduction of Graph Neural Networks (GNNs) [Kipf and Welling, 2016a] and autoencoders (AEs), many studies [Kipf and Welling, 2016a] [Grover *et al.*, 2019] have used GNNs and AEs to encode to and decode from latent representations. Many autoencoder-based graph generation models, like Variational Auto-Encoders (VGAE), GraphVAE, and MolGAN. These models can be used in graph data imputation problems since they deal with both graph feature generation and structure generation. GraphUnet [Gao and Ji, 2019] proposed a U-net-like graph autoencoder, which we chose as our base graph autoencoder. GraphUnet introduces the conceptions of graph pooling for summarizing a graph to a small-size graph latent space and graph unpooling for recovering the small graph latent space to the original graph topology. We use ASAPool [Ranjan *et al.*, 2020] instead of the graph pool layer in Graph-Unet.

$$\begin{aligned} \mathbf{y} &= \text{LEConv}(\mathbf{X}, \mathbf{A}), \mathbf{idx} = \text{top}_k(\mathbf{y}) \\ \mathbf{X}' &= (\mathbf{X} \odot \tanh(\mathbf{y}))_{\mathbf{idx}}, \mathbf{A}' = \mathbf{A}_{\mathbf{idx}, \mathbf{idx}}. \end{aligned} \quad (1)$$

The formula of unpooling operation [Gao and Ji, 2019]:

$$\mathbf{X}' = \text{distribute}(\mathbf{0}_{L \times C}, \mathbf{X}, \mathbf{idx}), \quad (2)$$

where $\mathbf{idx} \in \mathbb{Z}^k$ contains indices of selected nodes in the corresponding pool layer that reduces the graph size from L nodes to k nodes. $\mathbf{X}' \in \mathbb{R}^{k \times C}$ are the feature matrix of the current graph, and $\mathbf{0}_{L \times C}$ are the initially empty feature matrix for the new graph. $\text{distribute}(\mathbf{0}_{L \times C}, \mathbf{X}, \mathbf{idx})$ is the operation that distributes row vectors in \mathbf{X} into $\mathbf{0}_{L \times C}$ feature matrix according to their corresponding indices stored in \mathbf{idx} .

2.2 Adversarial Models

Our method is motivated by the generative adversarial network (GAN) [Goodfellow *et al.*, 2014]. GAN plays an adversarial game with two linked models: the generator G and the discriminator D . The discriminator discriminates if an input sample comes from the realistic data distribution or the generated data distribution. Simultaneously, the generator is trained to generate the samples to convince the discriminator that the generated samples come from the prior data distribution. G tries to generate samples to fool the discriminator, and D tries to differentiate samples correctly.

$$\begin{aligned} \min_G \max_D \mathcal{L}(D, G) = \\ \mathbb{E}_{x \sim p_{\text{data}}(x)} [\log D(x)] + \mathbb{E}_{z \sim p_z(z)} [\log(1 - D(G(z)))] \end{aligned} \quad (3)$$

To prevent undesired behavior such as mode collapse [Salimans *et al.*, 2016] and to stabilize learning, we use Two Time-scale Update Rule (TTUR) [Heusel *et al.*, 2017] and improved

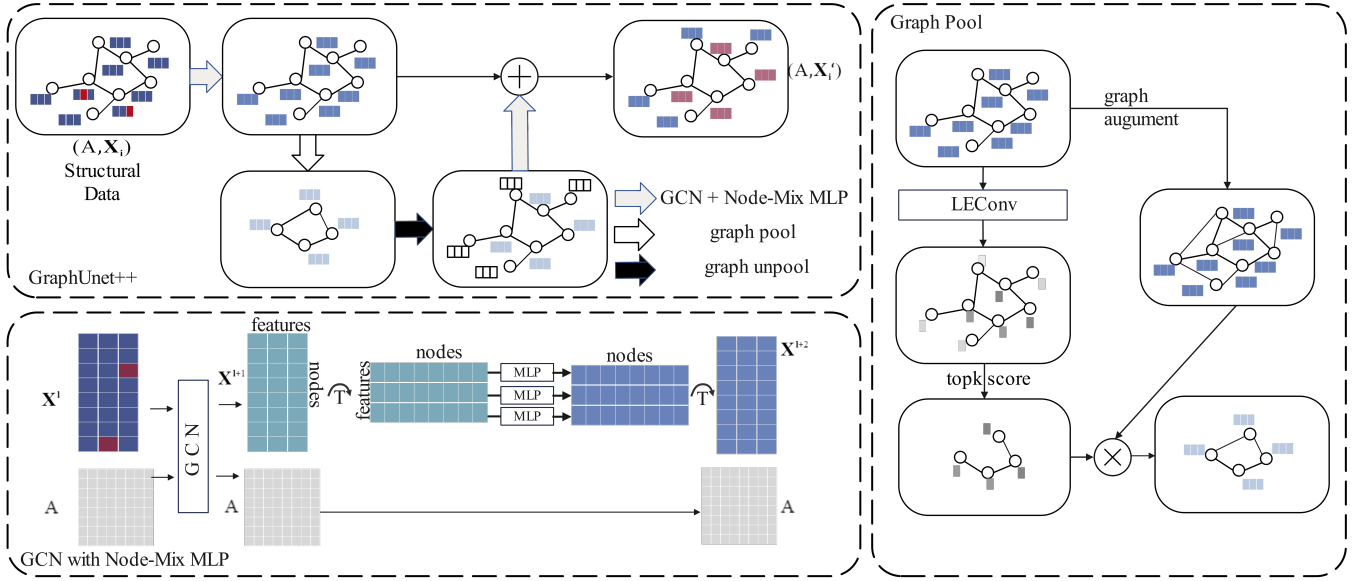


Figure 2: Overview of GraphUnet++: Incorporating graph convolutional layers, node-mix MLP, graph pooling, and graph unpooling. The combination of GCN and node-mix MLP is utilized to extract both global and local representations of the graph. The node-mix MLP facilitates information exchange between nodes, with parameter sharing across all layers. Graph pooling is executed using LEConv to calculate the impact score for each node in clusters, followed by selecting top-k score nodes and the maintaining connectivity of subgraphs. Unpooling involves putting the feature of pooled graph back to its original corresponding nodes.

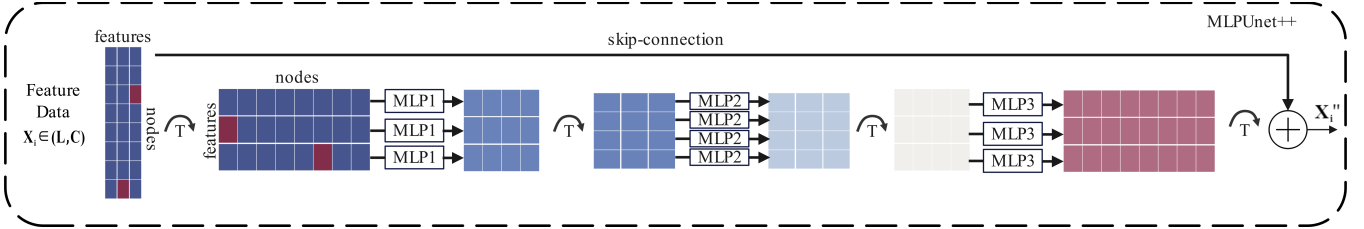


Figure 3: MLPUnet++ Network consists of node-mix MLPs and feature-mix MLPs, each consisting of two fully connected layers and a LeakyReLU nonlinearity. Skip-connections are also included.

WGAN [Gulrajani *et al.*, 2017], an alternative and more stable GAN model that minimizes a better-suited divergence. In our implementation, the formulation of adversarial loss is as follows:

$$\mathcal{L}_{wgan-gp} = \mathbb{E}_{\tilde{\mathbf{x}} \sim \mathbb{P}_{gen}} [D(\tilde{\mathbf{x}})] - \mathbb{E}_{\mathbf{x} \sim \mathbb{P}_{real}} [D(\mathbf{x})] + \lambda_{GP} \mathbb{E}_{\tilde{\mathbf{x}} \sim \mathbb{P}_{\tilde{\mathbf{x}}}} \left[(\|\nabla_{\tilde{\mathbf{x}}} D(\tilde{\mathbf{x}})\|_2 - 1)^2 \right], \quad (4)$$

where $\hat{\mathbf{x}}$ is a sampled linear combination between $x \sim p_{real}(x)$ and $\tilde{x} \sim p_{generated}(x)$, thus $\hat{x}_i = \epsilon x_i + (1 - \epsilon)\tilde{x}_i$ with $\epsilon \sim U(0, 1)$. The first two terms measure the Wasserstein distance between real and fake samples; the last term is the gradient penalty. As in the original paper, we set $\lambda_{GP} = 10$.

3 Problem Definition

In an undirected graph $G = (A; X)$, where $A \in \mathbb{R}^{N \times N}$ denotes the adjacency matrix and $X \in \mathbb{R}^{N \times D}$ denotes a comprehensive feature matrix. Here, X_{ij} represents the attribute of the i -th node in the j -th feature dimension on the

graph. In the context of graph attribute imputation, we define $R \in \{0; 1\}^{N \times D}$ as the mask matrix, where each element R_{ij} equals 1 if X_{ij} is observed and 0 otherwise.

This study aims to predict the missing graph attributes X_{ij} where $R_{ij} = 0$. In essence, we aspire to construct a mapping function $f(\cdot)$ that generates the imputed data matrix $\tilde{X} \in \mathbb{R}^{N \times D}$, formally defined as follows:

$$\tilde{X} = f(X; R; A). \quad (5)$$

4 Proposed Algorithm

4.1 Framework

We aim to train a resilient generator for a given graph $G = (A; X)$. We accomplish this by employing an adversarial architecture along with a graph autoencoder and MLPs autoencoder designed to process the entire graph directly and recover the missing rate. The overall workflow of DPGAN comprises two modules: the generator and the Subgraph discriminator.

4.2 Generator

The generator is comprised of an MLP (Multilayer Perceptron) autoencoder and a Graph autoencoder. Both leverage the graph structure A and the node content X as inputs to acquire a latent representation Z , and then they reconstruct the graph node features X using Z . Each autoencoder implements skip connections to construct a U-net architecture. The Graph autoencoder, built upon the Graph U-net structure, is employed to restore the signal via the graph structure. In contrast, the MLP autoencoder is mainly concentrated on numerical feature fitting. The output of the generator is the weighted sum of the two autoencoders.

Graph U-net++ The input and output of data imputation problems differ in parts of features, and both are renderings of the same graph structure. We design the generator architecture around these considerations. Therefore, we consider the generator with skips.

Numerous preceding studies [Li *et al.*, 2020] [Gao *et al.*, 2023] in this domain have employed an encoder-decoder network architecture. Within this framework, the input data is transformed into a latent space representation, from which features are subsequently reconstructed. A critical aspect of this approach is the necessity for information to traverse through all network layers, often resulting in a bottleneck. However, in many data imputation scenarios, a substantial portion of information is common to input and output. Therefore, it would be advantageous to facilitate the direct transfer of this shared information across the network, bypassing the bottleneck.

To facilitate the generator’s access to observed information, we incorporate skip-connections into its design, inspired by the “Graph U-Net” architecture [Gao and Ji, 2019]. While closely following the original Graph U-Net framework, our model diverges in one critical aspect: we introduce node-mix MLP layers following the GCN, which are specifically designed to capture the long-range dependencies of nodes. Additionally, we replace the standard pooling layer with an Adaptive Structure Aware Pooling (ASAP) layer [Ranjan *et al.*, 2020]. This modification allows for more effective learning of hierarchical information. Our proposed architecture is named “Graph U-Net++”. The overview of GraphU-net++ is shown in Figure 2, and the formulation of Graph U-Net++ is as follows:

$$\tilde{X}' = \text{GraphU-net}++(X; R; A). \quad (6)$$

MLP U-net++ While Graph U-net can address the feature imputation problem, it can suffer from an oversmoothing issue, particularly when the network structure deepens, leading the network to lean towards low-frequency behaviors. To alleviate this problem, a model solely operating in the feature domain is needed to restore the lost high-frequency characteristics. This is achieved by employing a Multilayer Perceptron (MLP). The leading architecture substitutes the GCN part, as well as the pool and unpooling sections of the Graph U-net, with node-mix MLPs and feature-mixing MLPs respectively. The feature-mix MLPs are utilized, while the node-mix MLPs is employed to compress and expand the nodes’ information and increase the information exchange between each node and all other nodes. Figure 3 show the workflow

of MLPUnet++. And also the formulation of MLPUnet++ is:

$$\tilde{X}'' = \text{MLPUnet}++(X; R; A). \quad (7)$$

We use α to control the weights of the two channels. Therefore, the overall formulation for the generator is:

$$\tilde{X} = \alpha \text{MLPUnet}++(X; R; A) + (1 - \alpha) \text{GraphU-net}++(X; R; A) \quad (8)$$

4.3 Subgraph Discriminator

The subgraph discriminator compels recovered data to conform to a prior distribution through an adversarial training module, which discriminates whether the current recovered data $\tilde{X} \in \mathbb{R}^{N \times D}$ originates from the fake distribution or the prior distribution.

It is well known that as the number of GCN layers increases, the recovered features tend to be dominated by low frequencies. In order to recover a high-frequency signal, it is sufficient to restrict our attention to the structure in the local graph. Therefore, we design a subgraph discriminator architecture – inspired by the patch discriminator from [Isola *et al.*, 2017] – that only penalizes the scale of the subgraph. The subgraph size is controlled by the number of graph pooling layers in the network. This discriminator attempts to classify whether each subgraph in a graph is real or fake.

Furthermore, adversarial training necessitates that the capabilities of two modules, the generator and the discriminator, be on par. This is particularly crucial given that GNN-based generators often exhibit limited feature restoration ability. By allowing the discriminator to adjust its focus on subgraphs of varying sizes, we introduce a level of flexibility in the discriminator’s capacity. One-hop subgraph discriminator, as shown in Figure 4, will focus on the fidelity subgraph. The smaller number of hops implies more detailed observation, enabling a more nuanced analysis that is impossible with a single output per graph, which can easily overlook subtle details. Specifically, the zero hop subgraph discriminator or node discriminator means will output a fidelity score for each node.

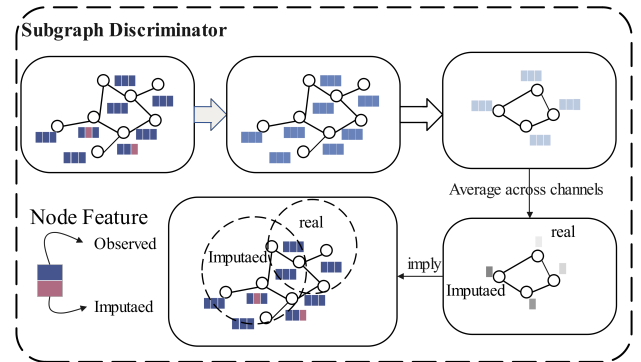


Figure 4: Subgraph Discriminator: Following one graph convolution layer with a node-mix layer and one graph pooling layer, the graph size is reduced to 4 nodes. Each node represents the fidelity of the subgraph in its position.

Method	ENZYMES	QM9	Synthie	FRANKE	FIRST_DB	ENZYMES
	RMSE with 0.1 missing features					ACC.
MEAN	0.0602	0.2983	0.2063	0.3891	0.1500	65.06%
KNN[Zhang, 2012]	0.0350	0.3058	0.1718	0.2010	0.1296	63.53%
SVD [Troyanskaya <i>et al.</i> , 2001]	0.0783	0.2524	0.1697	0.2766	0.1685	61.60%
MICE [Buuren, 2011]	0.0292	0.1986	0.1899	0.1359	0.1036	64.46%
GAIN [Yoon <i>et al.</i> , 2018]	0.0300	0.1973	0.1649	0.1103	0.0909	64.42%
OT [Muzellec <i>et al.</i> , 2020]	0.0323	0.2003	0.1865	0.1116	0.0892	64.13%
MIRACLE [Kyono <i>et al.</i> , 2021]	0.0288	0.1846	0.1632	0.1196	0.0889	65.03%
GraphVAE [Simonovsky, 2018]	0.0357	0.1579	0.1898	0.1099	0.1202	63.46%
MolGAN [De Cao and Kipf, 2018]	0.0326	0.1478	0.1864	0.1078	0.1379	64.16%
GRAPE [You <i>et al.</i> , 2020]	0.0302	0.1869	0.1798	0.1069	0.0986	64.48%
GDN [Li <i>et al.</i> , 2020]	0.0268	0.1598	0.1764	0.1066	0.0869	65.57%
MEGAE [Gao <i>et al.</i> , 2023]	<u>0.0223</u>	<u>0.1396</u>	<u>0.1203</u>	<u>0.0936</u>	<u>0.0789</u>	<u>66.27%</u>
DPGAN (ours)	0.0193	0.1011	0.1069	0.0908	0.0757	67.34%
Performance gain	0.0030	0.0385	0.0134	0.0028	0.0032	1.07%
	0.0409	0.2047	0.0994	0.2983	0.0928	5.74%

Table 1: RMSE results on five multi-graph datasets. After running five trials with random seed, we report the mean results in which the best method is bolded and the second best is underlined. Performance gains indicate the maximum (lower) and minimum (upper) gains of state-of-the-art (DPGAN) compared to other baselines. Note that we abbreviate 'FRANKENSTEIN' and 'FIRSTMM.DB' to 'FRANKE' and 'FIRST_DB', respectively.

4.4 Optimization

The overall training loss is defined as:

$$\mathcal{L} = \mathcal{L}_{WGAN-GP} + \lambda_R \mathcal{L}_{\mathcal{R}} \quad (9)$$

where $\mathcal{L}_{WGAN-GP}$ is the adversarial loss, $\mathcal{L}_{\mathcal{R}}$ is reconstruction loss and λ_R is a hyperparameter to balance the regularization of adversarial loss and reconstruction loss, we choose λ_R from $\{1, 10, 100\}$.

In order to address the imputation precision, we introduce reconstruction Loss $\mathcal{L}_{\mathcal{R}}$. We follow the mean square loss for previous work [Li *et al.*, 2020] [Gao *et al.*, 2023]. In order to recover high-frequency signal [Isola *et al.*, 2017], we also try L1 loss in the ablation study.

$$\mathcal{L}_{\mathcal{R}} = \left\| (\mathbf{X} - \tilde{\mathbf{X}}) \odot (\mathbf{1}_{N \times D} - \mathbf{R}) \right\|_2 \quad (10)$$

5 Experiment

In this section, we validate the performance of DPGAN using a variety of datasets. We evaluate the effectiveness of DPGAN on two categories of graph datasets:

- **Imputation on multi-graph datasets.** We impute the missing graph attributes on multi-graph datasets, e.g., molecules and proteins. In addition, we report graph classification performance on graphs with imputed features.
- **Imputation on single-graph datasets.** We impute the missing values on single-graph datasets, e.g., social networks. We report RMSE on the graph with imputed features.

5.1 Imputation on Multi-graph Datasets

Datasets

We conduct experiments on five benchmark datasets [Morris *et al.*, 2020] from different domains: (1) bioinformatics, i.e., ENZYMES [Schomburg *et al.*, 2004]; (2) chemistry, i.e., QM9 [Ramakrishnan *et al.*, 2014] and FIRSTMM_DB [Neumann *et al.*, 2013]; (3) computer vision, i.e., FRANKENSTEIN [Neumann *et al.*, 2013]; (4) synthesis, i.e., Synthie [Morris *et al.*, 2016]. Details of these datasets are summarized in Table 2.

Datasets	Mean Nodes	Mean Edges	Features	Graph Number
ENZYMES	33	62	18	600
QM9	18	19	16	1290
Synthie	95	173	15	400
FRANKENSTEIN	17	18	780	4337
FIRSTMM_DB	1377	3074	1	41

Table 2: Summary of the experimental multi-graph datasets.

Baselines

We compare the performance of DPGAN against baselines in three categories: (1) statistical imputation methods including MEAN, KNN [Zhang, 2012] and SVD [Troyanskaya *et al.*, 2001]; (2) deep learning-based imputation models including MICE [Buuren, 2011], GAIN [Yoon *et al.*, 2018], OT [Muzellec *et al.*, 2020] and MIRACLE [Kyono *et al.*,

Method	Cora (RMSE)					CiteSeer (RMSE)				
	0.1 Miss	0.3 Miss	0.5 Miss	0.7 Miss	0.99 Miss	0.1 Miss	0.3 Miss	0.5 Miss	0.7 Miss	0.99 Miss
sRMGCNN[Monti <i>et al.</i> , 2017]	0.1180	0.1187	0.1193	0.1643	0.1837	0.0693	0.0745	0.1137	0.1163	0.1750
GC-MC[Berg <i>et al.</i> , 2017]	0.0995	0.1089	0.1292	0.1571	0.2352	0.0599	0.0865	0.1032	0.1248	0.1892
GRAPE[You <i>et al.</i> , 2020]	0.0975	0.1049	0.1256	0.1359	0.2274	0.0657	0.0930	0.1068	0.1295	0.1926
VGAE[Kipf and Welling, 2016b]	0.1105	0.1139	0.1616	0.2095	0.2892	0.0774	0.1060	0.1056	0.1350	0.2172
GDN[Li <i>et al.</i> , 2020]	<u>0.0946</u>	<u>0.0964</u>	<u>0.1085</u>	0.1332	0.2037	<u>0.0599</u>	<u>0.0895</u>	<u>0.0893</u>	0.1240	0.1784
MEGAE[Gao <i>et al.</i> , 2023]	0.0804	0.0849	0.0878	0.0941	<u>0.1208</u>	0.0567	0.0621	0.0741	0.0938	<u>0.1408</u>
DPGAN (ours)	0.1132	0.1124	0.1122	<u>0.1120</u>	0.1119	0.0950	0.0943	0.0944	0.0938	0.0931
Performance gain	-0.0328	-0.0275	-0.0244	-0.0179	0.0089	-0.0383	-0.0322	-0.0203	0.0000	0.0477
	0.0048	0.0063	0.0494	0.0975	0.1773	-0.0176	0.0117	0.0193	0.0412	0.1241

Table 3: Mean RMSE results of attribute imputation with different missing rates on Cora and CiteSeer. The best result is bolded and the second best is underline.

2021]; (3) graph learning-based models including GraphVAE [Simonovsky, 2018], MolGAN [De Cao and Kipf, 2018], GRAPE [You *et al.*, 2020], GDN [Li *et al.*, 2020], MEGAE [Gao *et al.*, 2023].

Setup

We use a 70-10-20 train-validation-test split and construct random missingness only on the test set. Each run has a different dataset split and the mask for feature missingness. After running for five trials, we report the Root Mean Squared Error (RMSE) results for imputation on the test set. For all baselines in ENZYMES, we use a 2-layer GCN for downstream classification. For hyperparameter tuning, we generally set the batch size to 128, except for the FIRST DB, which is set to 2. We select the number of hidden layers in the first GCN and MLP for both the Generator (G) and Discriminator (D) from the set {128, 256, 512, 1024}. Commonly, the combinations (256,256) and (1024,128) for the hidden layers of G and D, respectively, strike a good balance in their capabilities. For optimization, we use either Adam or SGD, and the initial alpha value is selected from {0.5, 0.7, 0.9}. As for learning rates, following the Two Time-Scale Update Rule[Heusel *et al.*, 2017], the learning rate of D rate is set to 0.04, while the learning rate of G is chosen from {0.01, 0.001, 0.0001}.

Results

Table 1 presents the experimental results with 10% missing features. These results demonstrate that our approach consistently achieves the lowest RMSE across all five datasets, surpassing the current state-of-the-art (SOTA) by margins ranging from 2.99% to 27.6%. The improvement of imputation also benefits the downstream classification task.

5.2 Imputation on Single-graph Datasets

Datasets

We assess DPGAN’s efficiency on two widely recognized datasets, which are citation network datasets—Cora, Citeseer [Sen *et al.*, 2008]. The detailed information of datasets is summarized in Table 4.

Datasets	Nodes	Edges	Features	Classes
Cora	2485	5069	1433	7
QM9	2120	3679	3703	6

Table 4: Summary of the experimental single-graph datasets.

Comparison Methods

For imputation performance, we benchmark DPGAN against leading methods like sRMGCNN [Monti *et al.*, 2017], GCMC [Berg *et al.*, 2017], GRAPE [You *et al.*, 2020], VGAE [Kipf and Welling, 2016b], GDN[Li *et al.*, 2020] and MEGAE[Gao *et al.*, 2023].

Experimental Framework

Our evaluation setup follows the previous work in [Gao *et al.*, 2023], primarily based on the approach by Kipf and Welling in 2017, where a standard dataset division is employed. Across all datasets, every iteration uses a distinct train-validation-test partition and a unique mask for random omissions in every feature dimension. After executing five trials, we present the average RMSE values for imputation.

Results

The experimental results for a single graph dataset are shown in Table 3. Due to the vast number of points and distinct features in these datasets, and given the constraints on computational resources, MLPUnet could not participate. We employed a single-channel GraphUnet combined with a node-level subgraph discriminator. We opted for the node-level subgraph because using different levels of subgraph discriminators here would lead to leakage in the training set. The results show that the single-channel DPGAN performs best for single-graph tasks with high missing rates. However, without MLPUnet, achieving excellent results at low missing rates is challenging.

5.3 Ablation Study

Objective Function and Generator Network

We conduct an ablation study on the QM9 and ENZYMES datasets. After running five trials, we report the average re-

sults in Table 5. From the outcomes, it is evident that the dual-channel generator outperforms the single-channel generator. Using the L2 distance to construct the reconstruction loss is superior to the L1 distance, except for the ENZYME dataset with low missing rates. Generators with residual connections are more effective than the no-skip connection encoder-decoder structures. Train autoencoders with adversarial loss prove to be better than those trained solely with reconstruction loss.

Methods	QM9	ENZYMES
<i>w/o</i> Graph Unet	0.1039	0.0224
<i>w/o</i> MLP Unet	0.1074	0.0509
<i>w/o</i> Skip Connection	0.1150	0.0483
<i>w/o</i> WGAN-gp	0.1192	0.0230
our method+ L_1	0.1209	0.0193
our method+ L_2	0.1011	0.0221

Table 5: Mean RMSE results of attribute imputation with different Generator structures and Objective functions on QM9 and ENZYMES. We also test our model under different reconstruction loss metrics. The best result is bolded.

From NodeDis to SubgraphDis to GraphDis

We examine the impact of changing our discriminator’s output subgraph by varying the discriminator’s depth, i.e., the number of graph pooling layers. This ranges from a node discriminator (NodeDis), which has no graph pooling layer, to a full Graph discriminator (GraphDis), which gets the final score by adding a fully connected layer in the output of 2-hop subgraphDis. "2-hop SubgraphDis" implies that the discriminator has two graph pooling layers. Notably, in this paper, the pooling rate for all graph pool operations is 0.5. The output of NodeDis retains the structure of the entire graph, and each node indicates the authenticity of that node. Hence, the authenticity of graph data is at the node level. This type of graph discriminator has been mentioned in [Spinelli *et al.*, 2020]. The output of GraphDis is a single authenticity score for an entire generated graph. This kind of single-value score structure has been seen in [De Cao and Kipf, 2018]. Table 6 presents the effects of using discriminators at different levels by measuring the RMSE of the previous dataset. It is important to note that elsewhere in this paper, unless otherwise mentioned, all experiments utilize a subgraph discriminator with two graph pooling layers (2-hop SubgraphDis).

It can be observed that using a subgraph discriminator, regardless of depth, can significantly enhance the effects of our GAN imputation data in the QM9 dataset. Employing a 1-hop SubgraphDis is enough to achieve a commendable RMSE. The 2-hop SubgraphDis, albeit slightly, achieves better scores. As we scale further, the poorer performance of NodeDis and GraphDis in QM9 is due to the fact that, during the training process, the generator struggles to counter a node-level discriminator; as such, a discriminator observes all nuances. On the other hand, a discriminator at the entire graph level can easily be bypassed, as the finer details get minimized in a single score.

Methods	QM9	ENZYMES
nodeDis	0.1593	0.01932
1-hop subgraphDis	0.1027	0.02576
2-hop subgraphDis	0.1011	0.02567
3-hop subgraphDis	0.1027	0.02691
graphDis	0.1581	0.02706

Table 6: Mean RMSE results of attribute imputation with different sizes of discriminator on QM9 and ENZYMES. The best result is bolded.

Thus, achieving a balance between the generator and discriminator is challenging. This can be achieved by controlling the pooling layers to adapt effectively to adversarial training across various graph datasets. Uniquely and notably in the ENZYME scenario, employing a 0-hop subgraph discriminator can yield enhanced results.

Imputation under various missing rates

Figure 5 shows that our proposed framework achieves high performance across various missing rates. Remarkably, it can effectively recover data even when all features are missing, a challenge that other algorithms have not addressed. Furthermore, as the missing rate decreases, the final α value increases, indicating that the specially designed MLPUnet++ plays a dominant role in the imputation process, particularly in scenarios with low missing rates. All the α values are initial at 0.5 and acquired after the training.

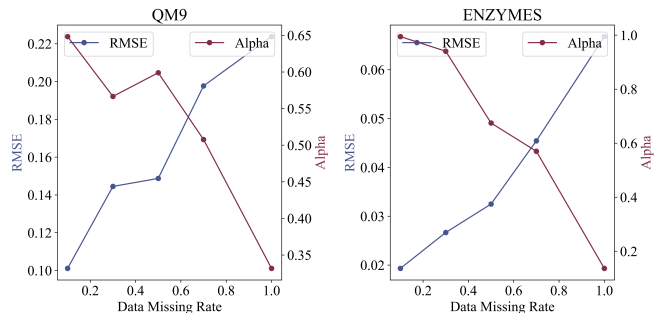


Figure 5: The imputation results under various missing rates. Our model is effective under various rates of data missing. Remarkably, it can reconstruct features relying solely on structure. As the rate of data missing varies, the final alpha value of the model also changes. A lower data missing rate results in a higher alpha value, indicating the dominant role of our designed MLPUnet.

6 Conclusion

This paper shows that dual-path autoencoders with subgraph adversarial regularization offer a promising approach for graph attribute imputation. The introduction of subgraph discriminators, which do not base their discrimination on a single value for evaluating a graph, enhances the training stability of graph-based GAN models, leading to better results in data imputation. The side-path Unet built on MLP further boosts the data imputation quality, although there are certain computational resource limitations.

References

- [Berg *et al.*, 2017] Rianne van den Berg, Thomas N Kipf, and Max Welling. Graph convolutional matrix completion. *arXiv preprint arXiv:1706.02263*, 2017.
- [Buuren, 2011] Van Buuren. mice: Multivariate imputation by chained equations in r. *Journal of statistical software*, 45:1–67, 2011.
- [De Cao and Kipf, 2018] Nicola De Cao and Thomas Kipf. Molgan: An implicit generative model for small molecular graphs. *arXiv preprint arXiv:1805.11973*, 2018.
- [Gao and Ji, 2019] Hongyang Gao and Shuiwang Ji. Graph u-nets. In *international conference on machine learning*, pages 2083–2092. PMLR, 2019.
- [Gao *et al.*, 2023] Ziqi Gao, Yifan Niu, Jiashun Cheng, Jianheng Tang, Lanqing Li, Tingyang Xu, Peilin Zhao, Fugee Tsung, and Jia Li. Handling missing data via max-entropy regularized graph autoencoder. In *Proceedings of the AAAI Conference on Artificial Intelligence*, volume 37, pages 7651–7659, 2023.
- [Goodfellow *et al.*, 2014] Ian J. Goodfellow, Jean Pouget-Abadie, Mehdi Mirza, Bing Xu, David Warde-Farley, Sherjil Ozair, Aaron Courville, and Yoshua Bengio. Generative adversarial networks, 2014.
- [Grover *et al.*, 2019] Aditya Grover, Aaron Zweig, and Stefano Ermon. Graphite: Iterative generative modeling of graphs. In *International conference on machine learning*, pages 2434–2444. PMLR, 2019.
- [Gulrajani *et al.*, 2017] Ishaan Gulrajani, Faruk Ahmed, Martin Arjovsky, Vincent Dumoulin, and Aaron C Courville. Improved training of wasserstein gans. *Advances in neural information processing systems*, 30, 2017.
- [Heusel *et al.*, 2017] Martin Heusel, Hubert Ramsauer, Thomas Unterthiner, Bernhard Nessler, and Sepp Hochreiter. Gans trained by a two time-scale update rule converge to a local nash equilibrium. *Advances in neural information processing systems*, 30, 2017.
- [Isola *et al.*, 2017] Phillip Isola, Jun-Yan Zhu, Tinghui Zhou, and Alexei A Efros. Image-to-image translation with conditional adversarial networks. In *Proceedings of the IEEE conference on computer vision and pattern recognition*, pages 1125–1134, 2017.
- [Kipf and Welling, 2016a] Thomas N Kipf and Max Welling. Semi-supervised classification with graph convolutional networks. *arXiv preprint arXiv:1609.02907*, 2016.
- [Kipf and Welling, 2016b] Thomas N Kipf and Max Welling. Variational graph auto-encoders. *arXiv preprint arXiv:1611.07308*, 2016.
- [Kyono *et al.*, 2021] Trent Kyono, Yao Zhang, Alexis Bellot, and Mihaela van der Schaar. Miracle: Causally-aware imputation via learning missing data mechanisms. *Advances in Neural Information Processing Systems*, 34:23806–23817, 2021.
- [Li *et al.*, 2017] Yaguang Li, Rose Yu, Cyrus Shahabi, and Yan Liu. Diffusion convolutional recurrent neural network: Data-driven traffic forecasting. *arXiv preprint arXiv:1707.01926*, 2017.
- [Li *et al.*, 2020] Jia Li, Tomas Yu, Da-Cheng Juan, Arjun Gopalan, Hong Cheng, and Andrew Tomkins. Graph autoencoders with deconvolutional networks. *arXiv preprint arXiv:2012.11898*, 2020.
- [Monti *et al.*, 2017] Federico Monti, Michael Bronstein, and Xavier Bresson. Geometric matrix completion with recurrent multi-graph neural networks. *Advances in neural information processing systems*, 30, 2017.
- [Morris *et al.*, 2016] Christopher Morris, Nils M Kriege, Kristian Kersting, and Petra Mutzel. Faster kernels for graphs with continuous attributes via hashing. In *2016 IEEE 16th International Conference on Data Mining (ICDM)*, pages 1095–1100. IEEE, 2016.
- [Morris *et al.*, 2020] Christopher Morris, Nils M Kriege, Franka Bause, Kristian Kersting, Petra Mutzel, and Marion Neumann. Tudataset: A collection of benchmark datasets for learning with graphs. *arXiv preprint arXiv:2007.08663*, 2020.
- [Muzellec *et al.*, 2020] Boris Muzellec, Julie Josse, Claire Boyer, and Marco Cuturi. Missing data imputation using optimal transport. pages 7130–7140, 2020.
- [Neumann *et al.*, 2013] Marion Neumann, Plinio Moreno, Laura Antanas, Roman Garnett, and Kristian Kersting. Graph kernels for object category prediction in task-dependent robot grasping. In *Online proceedings of the eleventh workshop on mining and learning with graphs*, pages 0–6, 2013.
- [Ni *et al.*, 2022] Qingjian Ni, Yuhui Wang, and Yifei Fang. Ge-stdgn: a novel spatio-temporal weather prediction model based on graph evolution. *Applied Intelligence*, pages 1–15, 2022.
- [Ramakrishnan *et al.*, 2014] Raghunathan Ramakrishnan, Pavlo O Dral, Matthias Rupp, and O Anatole Von Lilienfeld. Quantum chemistry structures and properties of 134 kilo molecules. *Scientific data*, 1(1):1–7, 2014.
- [Ranjan *et al.*, 2020] Ekagra Ranjan, Soumya Sanyal, and Partha Talukdar. Asap: Adaptive structure aware pooling for learning hierarchical graph representations. In *Proceedings of the AAAI Conference on Artificial Intelligence*, volume 34, pages 5470–5477, 2020.
- [Rossi *et al.*, 2022] Emanuele Rossi, Henry Kenlay, Maria I Gorinova, Benjamin Paul Chamberlain, Xiaowen Dong, and Michael M Bronstein. On the unreasonable effectiveness of feature propagation in learning on graphs with missing node features. In *Learning on Graphs Conference*, pages 11–1. PMLR, 2022.
- [Salimans *et al.*, 2016] Tim Salimans, Ian Goodfellow, Wojciech Zaremba, Vicki Cheung, Alec Radford, and Xi Chen. Improved techniques for training gans. *Advances in neural information processing systems*, 29, 2016.

- [Schomburg *et al.*, 2004] Ida Schomburg, Antje Chang, Christian Ebeling, Marion Gremse, Christian Heldt, Gregor Huhn, and Dietmar Schomburg. Brenda, the enzyme database: updates and major new developments. *Nucleic acids research*, 32(suppl_1):D431–D433, 2004.
- [Sen *et al.*, 2008] Prithviraj Sen, Galileo Namata, Mustafa Bilgic, Lise Getoor, Brian Galligher, and Tina Eliassi-Rad. Collective classification in network data. *AI magazine*, 29(3):93–93, 2008.
- [Simonovsky, 2018] Simonovsky. Graphvae: Towards generation of small graphs using variational autoencoders. In *Artificial Neural Networks and Machine Learning–ICANN 2018: 27th International Conference on Artificial Neural Networks, Rhodes, Greece, October 4-7, 2018, Proceedings, Part I 27*, pages 412–422. Springer, 2018.
- [Spinelli *et al.*, 2020] Indro Spinelli, Simone Scardapane, and Aurelio Uncini. Missing data imputation with adversarially-trained graph convolutional networks. *Neural Networks*, 129:249–260, 2020.
- [Taguchi *et al.*, 2021] Hibiki Taguchi, Xin Liu, and Tsuyoshi Murata. Graph convolutional networks for graphs containing missing features. *Future Generation Computer Systems*, 117:155–168, 2021.
- [Troyanskaya *et al.*, 2001] Olga Troyanskaya, Michael Cantor, Gavin Sherlock, Pat Brown, Trevor Hastie, Robert Tibshirani, David Botstein, and Russ B Altman. Missing value estimation methods for dna microarrays. *Bioinformatics*, 17(6):520–525, 2001.
- [Wieder *et al.*, 2020] Oliver Wieder, Stefan Kohlbacher, Méline Kuenemann, Arthur Garon, Pierre Ducrot, Thomas Seidel, and Thierry Langer. A compact review of molecular property prediction with graph neural networks. *Drug Discovery Today: Technologies*, 37:1–12, 2020.
- [Yomogida *et al.*, 2012] Yohei Yomogida, Jiang Pu, Hidekazu Shimotani, Shimpei Ono, Shu Hotta, Yoshihiro Iwasa, and Taishi Takenobu. Ambipolar organic single-crystal transistors based on ion gels. *Advanced Materials*, 24(32):4392–4397, 2012.
- [Yoon *et al.*, 2016] Jinsung Yoon, Camelia Davtyan, and Michaela van der Schaar. Discovery and clinical decision support for personalized healthcare. *IEEE journal of biomedical and health informatics*, 21(4):1133–1145, 2016.
- [Yoon *et al.*, 2018] Jinsung Yoon, James Jordon, and Michaela Schaar. Gain: Missing data imputation using generative adversarial nets. In *International conference on machine learning*, pages 5689–5698. PMLR, 2018.
- [You *et al.*, 2020] Jiaxuan You, Xiaobai Ma, Yi Ding, Mykel J Kochenderfer, and Jure Leskovec. Handling missing data with graph representation learning. *Advances in Neural Information Processing Systems*, 33:19075–19087, 2020.
- [Zhang, 2012] Shichao Zhang. Nearest neighbor selection for iteratively knn imputation. *Journal of Systems and Software*, 85(11):2541–2552, 2012.